Biochimica et Biophysica Acta 1838 (2014) 1931–1940

Contents lists available at ScienceDirect

Biochimica et Biophysica Acta

journal homepage: www.elsevier.com/locate/bbamem

Unusual penetration of phospholipid mono- and bilayers by *Quillaja* bark saponin biosurfactant

Kamil Wojciechowski [a,*], Marta Orczyk [a], Thomas Gutberlet [b], Marcus Trapp [b], Kuba Marcinkowski [a], Tomasz Kobiela [a], Thomas Geue [c]

[a] Faculty of Chemistry, Warsaw University of Technology, Noakowskiego 3, 00-664 Warsaw, Poland
[b] Helmholtz-Zentrum Berlin für Materialien und Energie GmbH, Hahn-Meitner-Platz 1, 14109 Berlin, Germany
[c] Laboratory for Neutron Scattering, Paul Scherrer Institute, WHGA/110, 5232 Villigen – PSI, Switzerland

ARTICLE INFO

Article history:
Received 10 January 2014
Received in revised form 31 March 2014
Accepted 7 April 2014
Available online 16 April 2014

Keywords:
QBS
DPPC
Surface rheology
Neutron reflectivity
QCM

ABSTRACT

The interactions between a model phospholipid 1,2-dipalmitoyl-sn-glycero-3-phosphocholine (DPPC) and a biosurfactant *Quillaja* Bark Saponin (QBS) obtained from the bark of *Quillaja* saponaria Molina were studied using simple models of biological membranes. QBS is known to interact strongly with the latter, exerting a number of haemolytic, cytotoxic and anti-microbial actions. The interaction of QBS dissolved in the subphase with DPPC monolayers and silicon-supported bilayers was studied above the cmc (10^{-3} M). Surface pressure relaxation and surface dilatational rheology combined with quartz crystal microbalance (QCM) and neutron reflectivity (NR) were employed for this purpose. The DPPC-penetrating abilities of QBS are compared with those of typical synthetic surfactants (SDS, CTAB and Triton X-100). We show that the penetration studies using high surface activity (bio)surfactants should be performed by a subphase exchange, not by spreading onto the surfactant solution. In contrast to the synthetic surfactants of similar surface activity, QBS does not collapse DPPC mono- and bilayers, but penetrates them, improving their surface dilatational elastic properties even in the highly compressed solid state. The dilatational viscoelasticity modulus increases from 204 mN/m for pure DPPC up to 310 mN/m for the QBS-penetrated layers, while it drops to near zero values in the case of the synthetic surfactants. The estimated maximum insertion pressure of QBS into DPPC monolayers exceeds the maximum surface pressure achievable in our setup, in agreement with the surface rheological response of the penetrated layers.

1. Introduction

Saponins are natural glycosides consisting of sugar (glycone) and non-sugar parts (aglycone) linked by a glycosidic bond. Usually, they are classified on the basis of the nature of aglycone (triterpenoid or steroid) or number of sugar chains attached to the aglycone part (mono-, bis-, and tri-desmosides: with one, two and three glycones, respectively). Typically, saccharides found in saponin molecules are: glucose, galactose, xylose, rhamnose, arabinose and glucuronic acid [1–3].

The Chilean tree *Quillaja saponaria* Molina and Californian tree *Yucca schidigera* are currently the most popular sources of saponins for commercial applications [4], which include foaming agents, emulsifiers, nutraceuticals, cholesterol lowering agents, and even immunological adjuvants [5]. It should be stressed here that the commercial products rarely contain a single compound with a well-defined structure. For example, the bark of *Quillaja saponaria* Molina contains at least 60 different saponins (mostly bisdesmoside triterpenoids) identified using mass spectrometry [4,6] and their content will vary in the final product depending on the source and employed method of purification [7]. Even for the most demanding pharmaceutical applications, mixtures of saponins are used. For example, the famous *Quil-A* saponin used for immunostimulating complexes (ISCOMS) has been found to contain at least four different components. The least toxic of them, QS-21, a potential human vaccine adjuvant, despite being initially a single compound, spontaneously isomerises and undergoes slow hydrolysis upon storage in water [8].

Although saponins are best known for their surface activity, many of them have cytotoxic and haemolytic properties. Especially the latter substantially hinder exploitation of other, beneficial properties of saponins on larger scales. Strong membrane activity of these compounds is probably related to the fact that they play essential roles in the defence systems of host plants and are usually found in large quantities in the tissues most susceptible to attack by fungi, bacteria and insecticides (root, tuber, bark, leaves, seeds and fruits) [9]. A plausible mechanism of biological action of saponins involves their interaction with lipid components of cell membranes, especially with cholesterol embedded in phospholipid bilayers of plasma membranes of the eukaryotes [10]. Moreover, saponins were shown to assist other molecules (e.g., a small, type I ribosome inactivating protein, saporin, [11,12], or even

* Corresponding author.
E-mail address: kamil.wojciechowski@ch.pw.edu.pl (K. Wojciechowski).

http://dx.doi.org/10.1016/j.bbamem.2014.04.008
0005-2736/

relatively large β-lactoglobulin [13]) in entering the cytosol without affecting the integrity of the plasma membranes.

While cholesterol seems to play essential role in the lysis of membranes of model and real erythrocytes by saponins [14–18], some triterpene saponins were shown to disrupt model phospholipid membranes in liposomes even in the absence of cholesterol [19]. The unusual effect of saponins on lipid monolayers was noted already by Schulman and Rideal already in 1937 [20]. They observed penetration of lecithin films by a "saponin" (unfortunately no details on its origin were provided) below the surface pressure of 22 mN/m.

Thus, before analysing the details of interaction between saponins and cholesterol embedded into phospholipid mono- and bilayers, we considered it useful to first analyse the saponin-phospholipid interactions. This work provides details of interactions in Langmuir monolayers and supported bilayers between a representative saponin, QBS (obtained from Sigma, cat. no. 84510) and a model phospholipid, DPPC [21,22] (see Fig. 1 for the structures).

2. Experimental

All solutions were prepared in Milli-Q water (Millipore), whose surface purity was verified by monitoring its dynamic surface tension with a drop shape analysis tensiometer PAT-1 (Sinterface, Germany). All glassware was cleaned with acetone and Hellmanex II solution (Hellma Worldwide) and subsequently rinsed with copious amounts of Milli-Q water. Dynamic surface tension of the water from the last rinsing was used to verify the surface purity of the glassware.

The surface pressure (Π) and surface dilatational rheology measurements were performed at constant temperature (21 °C) controlled with a thermostatic bath using a small Langmuir-Blodgett trough from KSV, Finland.

2.1. Chemicals

Zwitterionic phospholipid 1,2-dipalmitoyl-*sn*-glycero-3-phosphocholine (DPPC) was purchased from Sigma Aldrich with purity of 99% and stored at −20 °C. Spreading solution was prepared by dissolving DPPC in chloroform (*pure p.a.*) purchased from CHEMPUR (Poland). The experiments were performed with different types of synthetic surfactants: anionic – sodium dodecyl sulphate, SDS (Sigma 71725, purity ≥ 99.0%, CMC = $8{\cdot}10^{-3}$ M); cationic – cetyltrimethylammonium bromide, CTAB (Sigma 57-09-0, purity ≥ 99.0%, CMC = $9{\cdot}10^{-4}$ M) and non-ionic Triton X-100 (Sigma 9002-93-1, SigmaUltra, CMC = $2{\cdot}10^{-4}$ M), as well as an anionic biosurfactant *Quillaja* bark saponins QBS (Sigma 84510, Premium quality, 8–20% sapogenins, CMC = $1{\cdot}10^{-4}$ M). For the reasons explained in the Introduction, to avoid confusion with other saponin products, the QBS used in this study will be hereafter referred to as "Sigma" QBS.

2.2. Langmuir monolayers

The trough was filled with ultrapure water as a subphase. In each experiment 25 μl of DPPC dissolved in chloroform (0.34 mg/ml) was spread on the aqueous surface with a Hamilton syringe, and the chloroform was allowed to evaporate (15 min) before the measurements commenced.

All subphase exchange experiments were run with a Gilson's MINPULS 3 peristaltic pump. The outlets of the pump were connected to the Langmuir trough via Teflon tubing. The surfactant solution for exchange with the water subphase was dissolved into a flask at a concentration adjusted to reach the requested final concentration in the subphase (typically 10^{-3} M). Both inlet and outlet tubings were connected to the same pump head to assure the same flow rates, set to 2 ml/min.

For the surface pressure relaxation experiments, a monolayer prepared from DPPC as described above was spread on pure Milli-Q water. After the solvent evaporation the monolayer was compressed to the surface pressure of 32.5 mN/m (where the molecules in monolayer are believed to exhibit molecular packing similar to that estimated in phospholipid bilayers). The position of the barriers was then maintained and the evolution of surface pressure was monitored, typically for 1 hour. For the relaxation experiments on different subphases (surfactant solutions), the water was exchanged with concentrated solutions of the respective surfactants by a peristaltic pump with the flow rate of 2 ml/min, immediately after the solvent evaporation (15 min).

2.3. Surface dilatational rheology

The dilatational visco-elasticity modulus |E|, is defined as follows:

$$|E| = -\frac{d\pi}{dA} \cdot A$$

where A is the mean molecular area at a given surface pressure π.

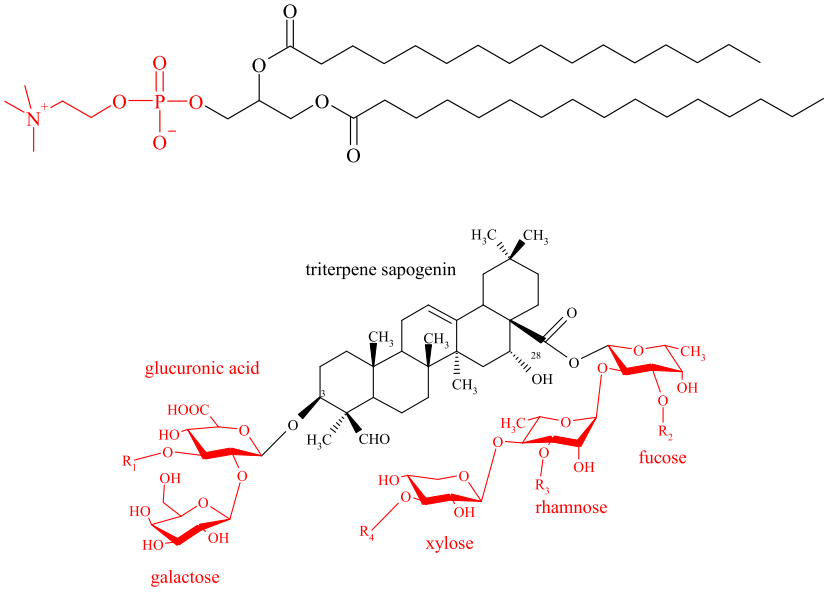

Fig. 1. Chemical structures of DPPC and QBS used in this work. R_1–R_4 — H or alkyl groups. The hydrophilic parts are highlighted in red.

The dilatational surface rheology response was probed at the frequency of 0.1 Hz, with the relative amplitude of 5% using an oscillating barrier method. Harmonic oscillations were applied at the end of each relaxation measurement. The $\Pi(t)$ amplitude and the phase shift with respect to the generated oscillations were obtained from the Fourier transformation of the data, and were used to calculate the real (E') and imaginary (E'') parts of the surface dilatational viscoelasticity modulus, $|E|$, [23]

$$E(\omega) = E'(\omega) + iE''(\omega)$$

2.4. Neutron reflectivity (NR)

In a reflectivity measurement the beam intensity, R, reflected from a surface, normalised to the incoming intensity at a certain angle of incidence, θ is recorded. In case of a neutron reflectivity (NR) experiment, R defined as above is measured as a function of scattering wave vector, q, expressed as the incidence angle θ normalised to the corresponding wavelength, λ, as $q = 4\pi \sin(\theta)/\lambda$. NR measurements were performed at the time-of-flight neutron reflectometer AMOR (Paul Scherrer Institute (PSI), Villigen, Switzerland) and BioRef (Helmholtz Zentrum Berlin (HZB), Berlin, Germany). The time-of-flight method allows the recording of a wide range of q values in a single angular setting.

The NR experiments at air/water interface were performed at AMOR time-of-flight neutron reflectometer [24] at three angles of incidence (0.25°, 0.65° and 1.4°) using a wavelength band from 3 to 12 Å, covering the necessary q range for the experiments of $q_{zmin} = 0.01$ Å^{-1} to $q_{zmax} = 0.15$ Å^{-1}. The resolution was set by a slit system on the incident side and the time-of-flight parameters to $\Delta q_z = 0.006$ Å^{-1}. A beam of rectangular cross section 1×35 mm^2 (for low angles) impinged on the samples at the air/water Langmuir trough. The scattered neutrons were recorded with a [3]. He-single detector tube in time-of-flight mode requiring typically 8 h of beam time.

The NR and ATR-IR experiments at Si/water interface were performed at the BioRef time-of-flight neutron reflectometer [25] using similar parameters as in the measurements at the air/water interface. The selected wavelength resolution was $\Delta\lambda/\lambda = 7\%$. Due to the operation of the choppers in an optical blind mode [26], the resulting wavelength resolution is constant. In order to cover the full q-space, three angles, namely 0.5°, 1.5° and 3.7° were used. With a chopper speed of 25 Hz and a resulting wavelength band of 2–16 Å, a q-range from 0.007–0.35 Å^{-1} was covered. In order to allow a simultaneous recording of FTIR-ATR spectra, a Bruker Vertex 70 spectrometer was mounted to the instrument, with the spectral resolution set to 4 cm^{-1}.

The DPPC bilayers were deposited onto Si block for NR experiments by spin coating of the chloroform solution (2 mg/ml). This procedure yields an oligolamellar lipid coating of the silicon substrate after the solvent evaporates, as a result of exposition to humidity from air [27]. Upon exposition to excess water the weakly bound outermost bilayers detach, as shown in [27,28]. Indeed, after hydration with D_2O in the NR cell, the NR profile was consistent with a single DPPC bilayer (see details in the Results section). The DPPC coated wafer was incubated with QBS solution of 10^{-3} M at 20 °C. Afterwards the subphase was exchanged with pure D_2O.

The experimentally obtained reflectivity curves were analysed by applying the standard fitting routine, using the Parratt 32 software [29]. It determines the optical reflectivity of neutrons from planar surfaces using a calculation based on Parratt's recursion scheme for stratified media [30]. The reflecting interface is modelled as consisting of layers of specific thickness, scattering length density and roughness, which are the fitting parameters. The neutron scattering length density (SLD) is defined by the sum of the bound coherent scattering length b_c of the reflecting material normalised by the volume, v, as $SLD = \sum b_c/v$. The model reflectivity profile is calculated and compared to the measured data, then the model is recursively adjusted by a change in the fitting parameters to best fit the data.

2.5. Quartz crystal microbalance with dissipation monitoring (QCM-D)

QCM-D is an accurate measuring technique commonly employed for the study of Supported Lipid Bilayers, SLBs. A quartz crystal microbalance operates by electronically measuring the change in frequency of oscillation of a resonating quartz crystal sensor. The frequency change is inversely related to the change of mass of material adsorbed atop the sensor. Monitoring of the dissipation parameter allows for quantification of visco-elastic properties of the adsorbed material, which are later used in modelling of the output data.

For QCM-D experiments the bilayers were deposited onto the SiO_2 layer of the QCM sensor in situ by the vesicle fusion method, as described in [31,32]. The DPPC vesicles were prepared according to standard procedures. In brief, DPPC was dissolved in chloroform (0.2 mg/ml) and dried in a stream of nitrogen. The vesicles were obtained by hydrating the phospholipid film in Milli-Q water at 45 °C and extruded 31 times through a 100 nm polycarbonate Whattman filter using a Mini-Extruder (Avanti Lipids). The temperature of hydration and all the subsequent operations was chosen to lie above the chain melting (L_β/L_α phase transition) temperature, $T_m = 41$ °C for DPPC. The extruded vesicle suspensions were introduced into the measuring cell of QCM-D at a flow rate of 0.1 ml/min maintaining the temperature of 45 °C. The deposition of the vesicles onto SiO_2 was followed in real time by monitoring the frequency and dissipation response of the QCM-D sensor. After completion of the vesicle deposition procedure, the vesicle suspension was exchanged for Milli-Q water to rinse off the non-adsorbed DPPC material prior to introducing the QBS solution (10^{-3} M). At the end of the experiment the QBS solution was exchanged again for Milli-Q water in order to assess reversibility of the registered changes of frequency and dissipation. All operations and measurements were performed at 45 °C.

3. Results

3.1. Interaction of QBS with DPPC monolayer at air-water interface

In the first part of the study, the DPPC monolayers were used as the simplest model of a single leaflet of the phospholipid bilayer. Even though in such an approach the two leaflet (outer and inner) interactions cannot be taken into account, the simplicity of the experimental setup facilitates data collection and analysis.

3.2. Spreading a DPPC monolayer onto QBS solution vs. spreading onto pure water followed by the subphase exchange

The monolayer penetration studies can be performed either by spreading a monolayer directly onto the aqueous solution of a water-soluble surfactant, or by spreading onto pure water followed by subphase exchange. Despite the fact that the former method is experimentally simpler, the uneven surface pressure distribution during spreading and the presence of the spreading solvent may alter the interactions between the soluble and insoluble components of the mixed layers. To avoid these problems, for the purpose of this study we developed a setup for subphase exchange using a peristaltic pump connected to the Langmuir trough with Teflon tubing. This allowed us to continuously exchange the subphase without disturbing the surface. The constant volume of the subphase in the trough is maintained by using the same flow rate for the inflow and outflow. The concentration and volume of the QBS solution in the external container were chosen to produce the requested concentration in the trough after mixing. The tests with aniline blue dye dissolved in water proved that with typical experimental conditions employed in this study the exchange was complete after 15 min (see Fig. S1, supplementary material for the photographs).

The subphase exchange setup allowed to compare the surface pressure isotherm of DPPC spread on QBS solution (10^{-3} M) with that spread on pure water followed by the subphase exchange resulting in the same final concentration of QBS (10^{-3} M). In both cases the

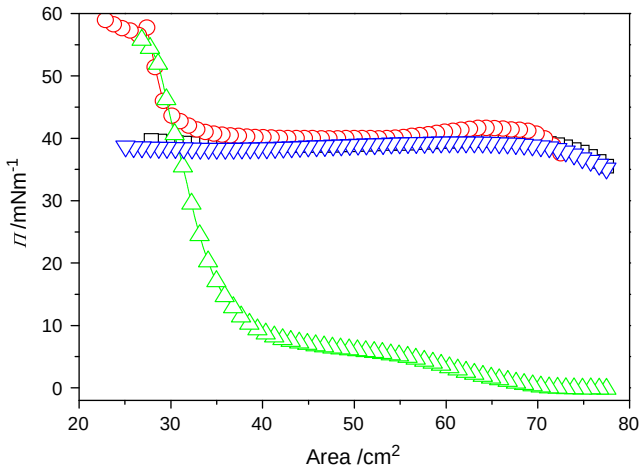

Fig. 2. Surface pressure – trough area isotherms for DPPC on 10^{-3} M QBS subphase. The phospholipid was spread either directly on QBS solution (□) or on water, which was subsequently exchanged for QBS after the spreading solvent evaporated (○). For comparison also the isotherms for DPPC on water (Δ) and for the Gibbs layer formed on 10^{-3} M QBS solution (▽), obtained under the same conditions, are shown.

compression started 60 min after spreading (15 min for the casting solvent evaporation + 45 min for subphase exchange or surface pressure equilibration). The two compression isotherms (presented as surface pressure vs area of the trough) are compared in Fig. 2, where also the analogous isotherms for DPPC on water and pure QBS (Gibbs layer, adsorbed during 1 h) are added for comparison.

The fact that the isotherm obtained for DPPC spread directly onto QBS practically coincides with that for bare QBS shows that the expected Langmuir monolayer is not formed when a monolayer-forming phospholipid is spread onto the surfactant-containing subphase. Instead, the phospholipid is probably entrapped in micelles in the surfactant subphase, and the layer formed consists mainly of spontaneously adsorbed QBS (Gibbs layer). In some systems, especially when the monolayer-penetrating molecules are not highly surface active, the direct spreading is applicable and produces reliable results [33]. However, in the case of highly surface active and fast adsorbing amphiphiles, we believe that the subphase exchange approach, as described above, is more appropriate.

3.3. Penetration of DPPC monolayers by water-soluble surfactants

The new setup allowing for subphase exchange was used to compare the dynamics of penetration of different surfactants into the DPPC monolayer compressed to the surface pressure, $\Pi_0 = 32.5$ mN/m. This value was chosen since it is believed to correspond to the lateral pressure in lipid bilayers of biological membranes [34]. Immediately after compressing the DPPC monolayers to Π_0, the subphase was exchanged for QBS, Triton X-100, CTAB or SDS and the surface pressure was monitored for 3600 s (Fig. 3). The final concentrations above the corresponding cmc values for all the surfactants were chosen (10^{-3} M for QBS, Triton X-100 and CTAB, and 10^{-2} M for SDS) to enable fast adsorption and to assure the presence of micelles in the subphase.

Both synthetic ionic surfactants employed in this study (SDS, CTAB) clearly induced the DPPC monolayer collapse, as opposed to QBS and

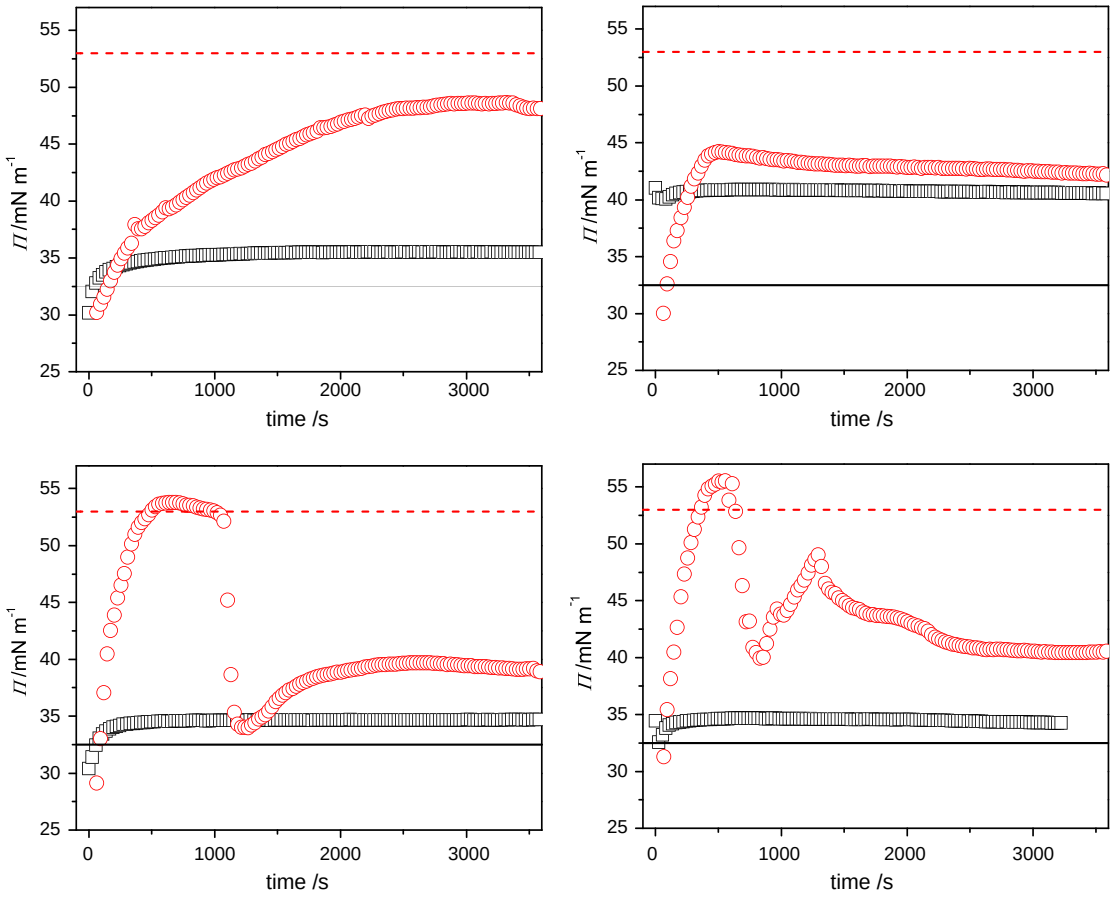

Fig. 3. Surface pressure relaxation for DPPC monolayers initially spread on water and compressed to $\Pi_0 = 32.5$ mN/m prior to the subphase exchange (○) against: QBS (10^{-3} M, upper left), Triton X-100 (10^{-3} M, upper right), CTAB (10^{-3} M bottom left), and SDS (10^{-2} M, bottom right). For comparison also the corresponding dynamic surface pressures for the pure surfactants are shown (□). The initial surface pressure ($\Pi_0 = 32.5$ mN/m) and the maximum surface pressure achievable in our setup for DPPC ($\Pi_{max} = 53$ mN/m) are shown as straight solid and dashed lines, respectively.

Triton X-100. In case of the ionic surfactants, the surface pressure increased abruptly within the first 10 min, i.e., even before the subphase exchange was complete. Soon after reaching the maximum surface pressure achievable in our setup for the pure DPPC monolayer ($\Pi_{max} = 53$ mN/m), a sudden drop of Π was observed, followed by some poorly reproducible oscillations, indicative of monolayer destruction. On the other hand, for Triton X-100 and QBS the increase of surface pressure was much less pronounced, so the maximum surface pressure was not reached. It is worth noting that for Triton X-100 the maximum pressure reached in the presence of DPPC monolayer was only slightly higher than that for the bare surfactant (41 mN/m), while for QBS the pressure stabilised some 13 mN/m above the level of the surfactant alone (35 mN/m). It should be stressed that the final surface pressure attained after penetration is not a simple function of the surface pressure attainable by the individual surfactant alone: QBS, CTAB and SDS in the absence of DPPC at the given concentrations reach almost the same surface pressure of about 35 mN/m, yet only the two synthetic surfactants induced the detrimental increase of Π in presence of DPPC. On the other hand, Triton X-100 which alone can attain higher surface pressure (41 mN/m) still could not compress the DPPC monolayer to such an extent as to collapse it.

3.4. Surface rheology of DPPC monolayers penetrated with water-soluble surfactants

The surface dilatational rheology analysis was performed for the pure DPPC, pure (bio)surfactants and mixed DPPC-surfactant (surfactant-penetrated) layers, directly after measuring the surface pressure relaxation. For this purpose, the Langmuir trough barriers were harmonically moved at the frequency of 0.1 Hz and the surface pressure response was analysed as described in the experimental part in order to obtain the elastic (E') and loss (E'') parts of the surface dilatational visco-elasticity modulus ($|E|$). From Table 1, collecting the corresponding E' and E'' values for pure components, it is clear that both insoluble DPPC and soluble (bio)surfactants layers (Langmuir and Gibbs, respectively) display predominantly elastic character in dilatation ($E' > E''$). Note that the slightly negative values of E'' obtained for CTAB and Triton X-100 are artefacts and should not be interpreted as negative viscosity of the layers.

To simplify the subsequent discussion, all the data will be presented as surface dilatational visco-elasticity modulus, $|E|$. The results are collected in Fig. 4, together with the corresponding values for the bare surfactants (in the absence of spread DPPC monolayer, i.e., for the Gibbs layers of the surfactants). For comparison, also the dilatational visco-elasticity modulus, $|E|$, for DPPC on pure water is shown. The latter values are in reasonable agreement with those reported by Miano et al. for DPPC monolayers spread on water drops [35] and Caro et al. [36], who reported the dilatational viscoelasticity modulus of about 280 mN/m at the same frequency and amplitude of oscillations (0.1 Hz, 5%, $\Pi_0 = 35$ mN/m), although for less aged interface (their measurements were performed just after the monolayer compression, without 1 hour delay as in our study). All the synthetic surfactants show very weak dilatational rheology response when adsorbed either on the bare water-air surface, or on the pre-existing DPPC monolayer

Table 1
Surface dilatational elasticity (E') and loss (E'') parts of the dilatational visco-elasticity modulus ($|E|$) for the spread DPPC monolayer compressed to $\Pi_0 = 32.5$ mN/m, and Gibbs layers formed by QBS (10^{-3} M), Triton X-100 (10^{-3} M), SDS (10^{-2} M) and CTAB (10^{-3} M) after 1 h relaxation on water at 21 °C.

Rheological parameter	Phospholipid	Surfactant			
	DPPC	SDS	CTAB	Triton X-100	QBS
E'/mN m^{-1}	185.1	1.4	1.7	0.9	138.6
E''/mN m^{-1}	86.5	0.5	−0.4	−0.1	7.9
$\|E\|$/mN m^{-1}	204.3	1.5	1.8	0.9	138.8

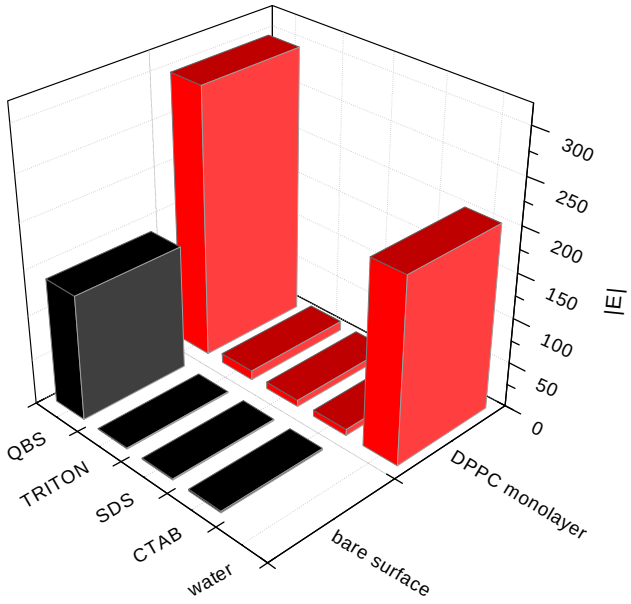

Fig. 4. Surface dilatational visco-elasticity modulus ($|E|$) of Gibbs layers formed on the surface of the surfactant solutions at concentrations above their cmc: QBS (10^{-3} M), Triton X-100 (10^{-3} M), SDS (10^{-2} M) and CTAB (10^{-3} M) compared with $|E|$ for the DPPC monolayers initially compressed to $\Pi_0 = 32.5$ mN/m measured after penetration by the same surfactants solutions. The corresponding value for DPPC on pure water is added for comparison.

compressed to $\Pi_0 = 32.5$ mN/m. Even though in the latter case $|E|$ takes slightly higher values than for the DPPC-free surface, they are still much lower than those for the DPPC spread on pure water. Hence, the rheological properties after 1 hour contact with CTAB, SDS and Triton X-100 resemble much more the adsorbed layers of the bare surfactants than those for the spread DPPC monolayer. This indicates that the DPPC monolayer after exposure to these surfactants disappears almost completely and the phospholipid is solubilized in their micelles within the subphase. The spread Langmuir layers of the phospholipid are simply expelled from the water surface by the adsorbing surfactants.

A distinctly different behaviour is observed for QBS, where an increase of $|E|$ can be noticed upon subphase exchange underneath the DPPC spread layer. This suggests that QBS does not simply replace DPPC, but instead incorporates into the monolayer, consequently enhancing its surface rheological response. It is worth noting that Triton X-100 shows a completely different rheological response than QBS (Fig. 4), even though both behave similarly in the surface pressure relaxation experiments (Fig. 3). Despite similar surface pressure relaxation behaviour (no indication of the monolayer collapse), the resulting mixed layer is characterised by a much lower dilatational visco-elasticity modulus values for Triton X-100 than for QBS.

3.5. Penetration of DPPC monolayers at the water/air interface by QBS

In order to better understand the unique interactions of QBS with DPPC monolayers, the effect of the initial surface pressure (and hence the phase of the monolayer) on the extent of QBS penetration was studied. The DPPC monolayer was first spread onto pure water and after solvent evaporation (15 min) it was compressed to the given Π_0, and the subphase exchange was initiated. The final QBS concentration was set to 10^{-3} M and the initial surface pressure values were chosen to correspond to the liquid expanded, LE (5 mN/m and 20 mN/m), liquid condensed, LC (32.5 mN/m), and solid (47 mN/m and 51 mN/m) phases. The highest value was chosen to lie just below that of the maximum surface pressure achievable in our setup for DPPC (53 mN/m) in order to verify whether QBS is capable of collapsing the DPPC layer at all. In all cases, the surface pressure was monitored during one hour and the

results are shown in Fig. 5 (a–e), together with the corresponding surface pressure relaxation for QBS in the absence of DPPC ($\Pi_0 = 0$).

First of all, although it is not acknowledged by many authors, the surface pressure of DPPC on pure water slightly decays after a quick compression to the given surface pressure, Π_0, even when the latter is set as low as 5 mN/m. In contrast, when QBS is present in the subsurface, the surface pressure increases for all Π_0. It is interesting to note that at short times the relaxation curves for the DPPC/QBS systems coincide with those for the DPPC/water. This is related to a finite rate of the subphase exchange: during the first ca. 100 s of the measurement the concentration of QBS is so low that the DPPC monolayer behaves as if it were present still on the surface of pure water. The final Π values increase with the increase of Π_0, for higher initial pressures they can even exceed the maximum surface pressure achievable in our setup for pure DPPC monolayers, $\Pi_{max} = 53$ mN/m (Fig. 5d). Only when the phospholipid monolayer was compressed to the state just below the maximum pressure for DPPC (51 mN/m), the relaxation curve showed some indication of a collapse (Fig. 5e). Surprisingly however, after some initial drop, the surface pressure started to rise again. Thus, despite the possible collapse, the DPPC layer in a highly compressed solid phase does not seem to be removed by QBS. In the resulting layer the phospholipid is still not completely replaced by the biosurfactant molecules, as in the case of the synthetic ionic surfactants described above.

The surface pressure relaxation results for different initial surface pressures were used to estimate the maximum insertion pressure (MIP), i.e., the maximum value of the surface pressure above which QBS would not be able to penetrate the DPPC monolayer. For this purpose, the increment of the surface pressure induced by addition of QBS ($\Delta\Pi$) was plotted as a function of the initial surface pressure, Π_0 (Fig. 5f). Although not enough data is available to quantify this effect, it seems that the slope of the $\Delta\Pi$ vs. Π_0 is different in different phase regions of the DPPC monolayer, in agreement with observations of Travkova and Brezesinski [33]. As noted by Calvez et al. [37] the MIP approach should be employed with care for the monolayers exhibiting phase transitions in the probed range of Π_0. Therefore for the purpose of this paper, only the data for the highest initial surface pressures (above 20 mN/m) were used for the extrapolation to $\Pi_0 = 0$, yielding the value of MIP = 57.3 mN/m.

3.6. Surface rheology of DPPC monolayers with QBS

The surface dilatational rheology results for DPPC layers penetrated by QBS at different Π_0 are collected in Fig. 6. In agreement with the surface relaxation data, for each Π_0 exposure of the DPPC layer to QBS results in more visco-elastic layer in dilatation, with the highest increase in $|E|$ observed for $\Pi_0 \leq 20$ mN/m. Interestingly, the increase of surface dilatational visco-elastic properties can be observed even for the highly compressed DPPC layers in the solid state ($\Pi_0 > 47$ mN/m). This clearly proves that QBS can penetrate into and increase the dilatational visco-elastic properties of even very dense DPPC layers, without disrupting

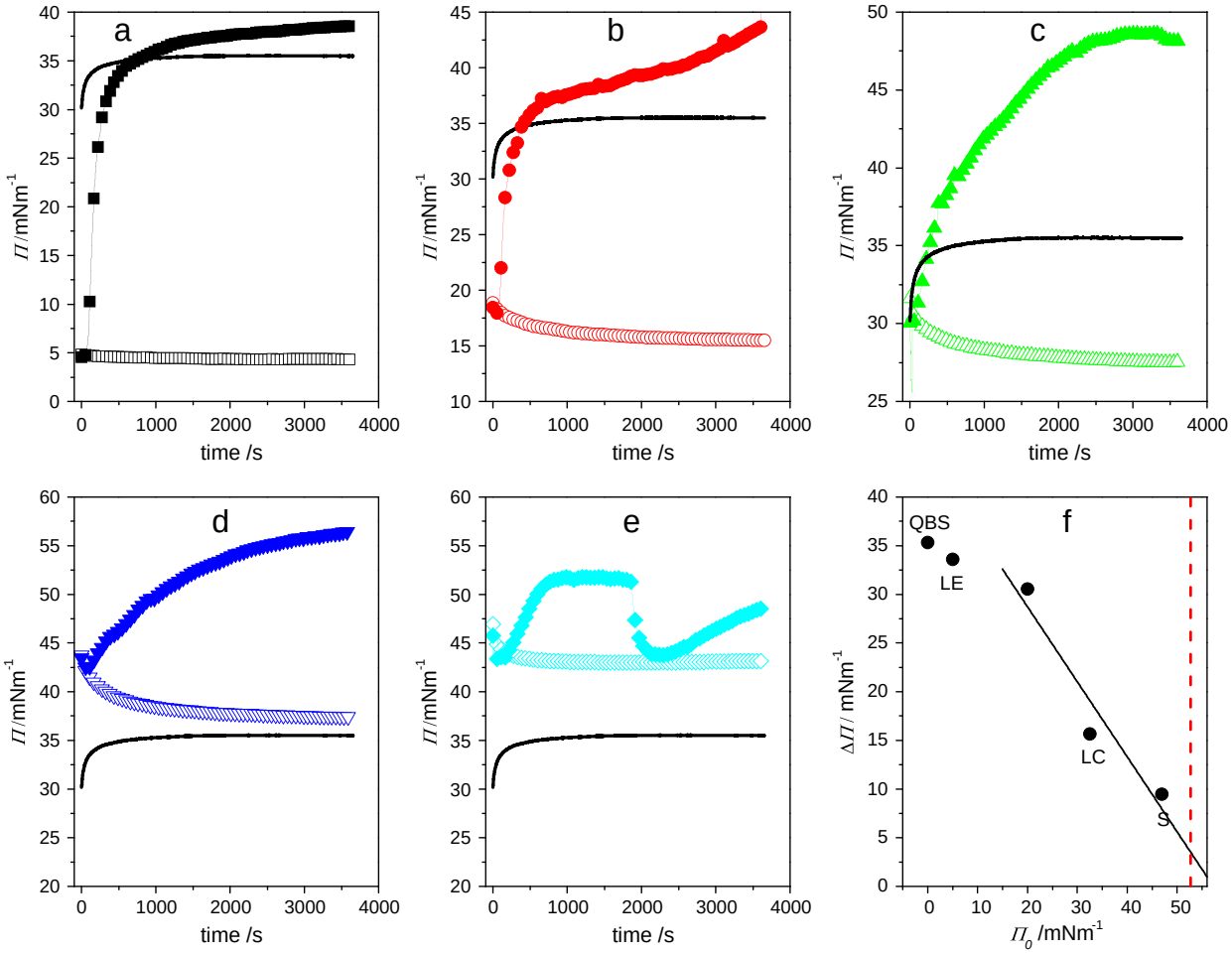

Fig. 5. Surface pressure relaxation for DPPC monolayers initially spread on water and compressed to different Π_0: 5 mN/m (a), 20 mN/m (b), 32.5 mN/m (c), 47 mN/m (d) and 51 mN/m (e) prior to the subphase exchange against 10^{-3} M aqueous solution of QBS (closed symbols). For comparison, also the corresponding relaxation curves on pure water (without subphase exchange) are shown (open symbols). The surface pressure development for 10^{-3} M solution of QBS (in the absence of DPPC monolayer) is shown as solid line on each graph to facilitate the comparison. $\Delta\Pi$ vs. Π_0 obtained from the graphs (a–e) is shown in graph (f). The maximum surface pressure achievable for DPPC in our setup is shown as a vertical dashed line (see the text for more details).

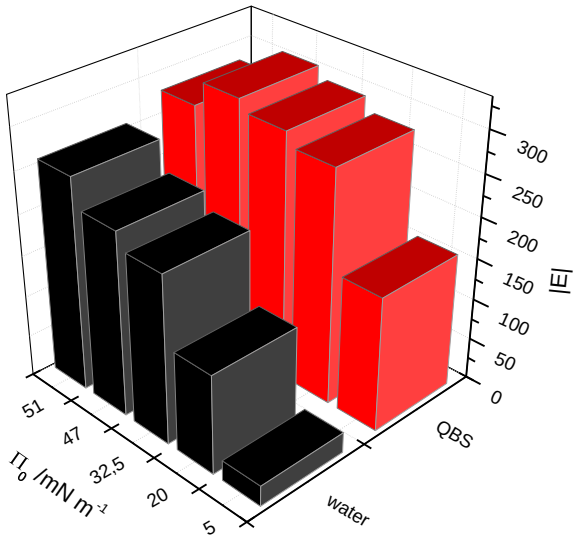

Fig. 6. Surface dilatational visco-elasticity modulus (|*E*|) of DPPC monolayers on water and penetrated by QBS (10^{-3} M) monolayers initially compressed to different Π_0.

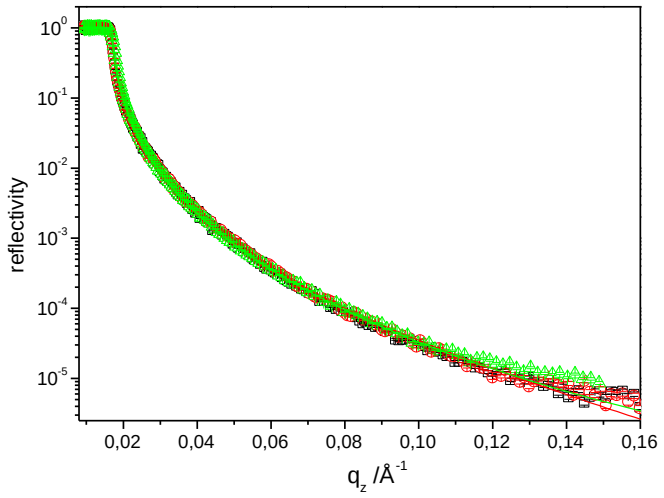

Fig. 7. Neutron reflectivity curve for bare DPPC monolayer compressed to $\Pi_0 = 32.5$ mN/m (black squares), the same DPPC monolayer penetrated with QBS, 10^{-3} M (red circles), and for a Gibbs layer formed by QBS (10^{-3} M) on bare air/D_2O interface (green triangles).

them. Only for the highest initial surface pressure, just below the maximum surface pressure achievable for DPPC in our setup (51 mN/m), the penetrating QBS molecules are capable of collapsing the monolayer structure. Nevertheless, even a so-damaged layer retains most of its dilatational elastic properties, as proven by only a slight reduction of the surface dilatational visco-elasticity modulus ($|E| = 280$ mN/m) with respect to the maximum value obtained for $\Pi_0 = 47$ mN/m ($|E| = 310$ mN/m). The value for $\Pi_0 = 51$ mN/m is still much higher than that for QBS layers with no DPPC (at $\Pi_0 = 0$), $|E| = 139$ mN/m, i.e., the value expected if DPPC was completely collapsed and replaced with QBS.

To assess the effect of the glycone (sugar) part of the QBS molecules on DPPC monolayer compressed to $\Pi_0 = 32.5$ mN/m, the effect of mono- and disaccharide (fructose and saccharose, respectively) at high concentration (0.5 M) was also analysed. The two sugars were chosen as they have been shown to fluidise phospholipid monolayers [38], albeit only at low surface pressures. Our results (see Figs S2-S3, supplementary information) show that both surface pressure and surface dilatational rheology response of the DPPC monolayers after 1 hour exposition to the highly concentrated sugar solutions are very similar to those on pure water. Therefore, even if they can penetrate the phospholipid monolayers at low surface pressures, in a more compressed state ($\Pi_0 = 32.5$ mN/m, as employed in the present study), the sugars alone are not retained in the DPPC monolayer.

3.7. Neutron reflectometry of DPPC monolayers with QBS

To gain knowledge on the structural changes of the DPPC monolayer interacting with QBS at the air/water interface, neutron reflectivity (NR) measurements were performed. The DPPC monolayer was first spread onto pure water and after solvent evaporation (15 min) it was compressed to the given Π_0 (32.5 mN/m, LC phase). Then QBS was added to the subphase to reach the QBS concentration of 10^{-3} M. Despite being controlled by processes slower than diffusion in the aqueous phase [7,39], the QBS adsorption at the flat DPPC monolayer is fast enough to establish equilibrium on the timescale shorter than necessary for setting up a NR measurement (the latter takes typically at least 20 min). The NR curves obtained for DPPC on water and on "Sigma" QBS overlapped significantly as shown in Fig. 7, suggesting that DPPC monolayer does not undergo significant changes upon penetration by QBS. Pure DPPC layer could be fitted reasonably using the literature values of scattering length density, $SLD = 3.10^{-6}$ Å^{-2} and thickness, $d = 9$ Å [40]. However, after contact with "Sigma" QBS the thickness of the adsorbed layer increased to $d = 29$ Å. At the same time the scattering length density also increased to $SLD = 4.8\ 10^{-6}$ Å^{-2}, suggesting more D_2O present within the layer. This behaviour is typical for adsorption of highly hydrated QBS molecules, as shown in our previous study [41]. It should also be noted that the NR curve for the Gibbs layer formed by QBS in the absence of DPPC differs from that obtained after adding QBS to the subphase underneath DPPC (Fig. 7), confirming that no displacement of the phospholipid by QBS takes place.

3.8. Interaction of QBS with DPPC bilayers at solid-water interface

Supported lipid bilayers (SLBs) can be considered better approximations of biological bilayer membranes than the monolayers. Therefore, studying the interaction of QBS with SLBs may yield information that can more easily be extrapolated to its interaction with real cell membranes.

3.9. QCM-D measurements of supported DPPC bilayers at the Si/water interface with QBS

The experiments using QCM-D were conducted in pure Milli-Q water to facilitate direct comparison with the results from the Langmuir trough. The supported lipid bilayers of DPPC were obtained by the vesicle fusion method [31,32], as described in the experimental part. The temperature in the measuring cell and that of all the media was maintained at 45 °C. Under these conditions (T = 45 °C, low ionic strength solvent), the DPPC bilayer formation proceeds via a mechanism of instant vesicle rupture upon adsorption to the substrate [42,43]. The formation of the bilayer is evidenced by the stabilisation of the frequency signal and the low values of dissipation registered by the QCM-D during the first 20 min (Fig. 8).

After rapid formation of the first DPPC bilayer (t = 20 min, arrow 1 in Fig. 8) deposition of some additional material was observed (20 < t < 60 min, arrows 1–2 in Fig. 8). Judging from the small decrease of frequency and significant increase of dissipation accompanying this process, it is likely an adsorption of intact vesicles on the DPPC bilayer which was formed during the first 20 min of the vesicle deposition. These loosely adsorbed vesicles were easily removed by rinsing with pure water (60 < t < 70 min, arrows 2–3 in Fig. 8), as evidenced by a sudden change of dissipation and frequency.

The successive introduction of QBS resulted in a slow (90 < t < 130 min, arrows 4–5 in Fig. 8) but significant decrease of frequency (~10 Hz), mirrored by the increase of dissipation (~$1{\cdot}10^{-6}$). Clearly,

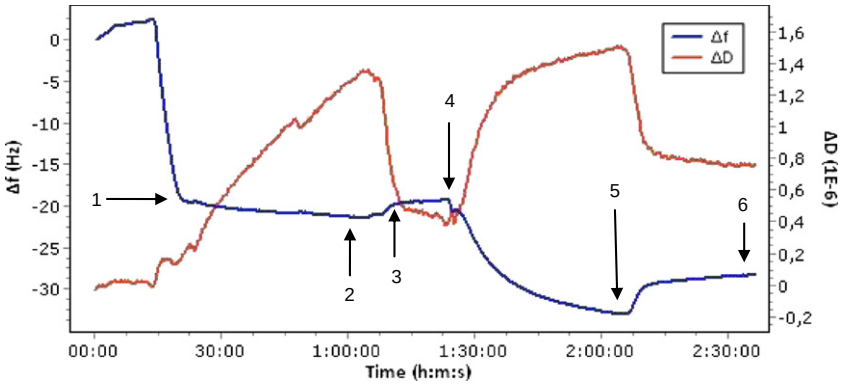

Fig. 8. Frequency and dissipation versus time for a typical QCM-D experiment conducted in Milli-Q water at 45 °C (data shown for the 5th overtone, see the text for more details).

some new material (most likely QBS molecules) was incorporated into the DPPC bilayer, significantly increasing its mass, but also altering its viscoelastic properties to a certain extent. After exchanging the QBS solution again for pure water, the trend of changes was partially reversed, with dissipation decreasing and frequency increasing ($130 < t < 160$ min, arrows 5–6 in Fig. 8). This shows that part of the previously adsorbed material was likely washed off, however the final frequency was still lower (~30 Hz) than that observed for the freshly-formed DPPC bilayer (thus the mass was higher).

3.10. Neutron reflectometry measurements of supported DPPC bilayers at the Si/water interface with QBS

The DPPC bilayer for NR study was deposited by spin coating the chloroform solution at room temperature on Si block. The reflectivity of the DPPC-covered silicon surface in D_2O as a function of the scattering vector, q (defined in the experimental part) is shown in Fig. 9 (black squares). This reflectivity profile could be well fitted to a model with two layers (D_2O underneath the bilayer and a single DPPC bilayer) with the thicknesses of $d_1 = 10$ and $d_2 = 48$ Å, respectively. The corresponding scattering length densities were $SLD_1 = 6.366{\cdot}10^{-6}$ and $SLD_2 = 1.6{\cdot}10^{-6}$ Å^{-2}. Next, the aqueous phase in the NR measuring cell was exchanged with a QBS aqueous solution (10^{-3} M) and the reflectivity was measured again (Fig. 9, red circles) showing that similarly to the DPPC monolayer, the bilayer is not removed by QBS. The main difference between the profiles before and after contact with "Sigma" QBS is the shoulder around 0.1 Å^{-1}, which becomes more pronounced upon penetration with QBS. The new reflectivity profile could be well fitted to the two-layer model with thickness of $d_1 = 14$ and $d_2 = 46$ Å, respectively. The corresponding scattering length densities were $SLD_1 = 6.366{\cdot}10^{-6}$ and $SLD_2 = 0.9{\cdot}10^{-6}$ Å^{-2}. The increased thickness of the water layer underneath the bilayer may suggest that some QBS molecules penetrated the bilayer and accumulated in the aqueous pool beneath it. The subsequent exchange of QBS solution back to pure D_2O resulted in practically the same curve as that before the incubation with QBS (green triangles, Fig. 9), suggesting that the process is almost completely reversible. This is not fully consistent with the QCM-D results, where even after rinsing with pure water some additional mass brought by QBS remained with the adsorbed layer. This difference stems probably from a lower sensitivity of NR to distinguish tiny changes in adsorption of highly hydrated QBS molecules. The corresponding FTIR-ATR spectra in the region of $-CH_2-$ and $-CH_3$ symmetric and asymmetric vibrations collected simultaneously with the NR experiments are shown in the inset of Fig. 9. The comparison of the IR spectra for bare DPPC with those after treatment with QBS (10^{-3} M) and its subsequent exchange for D_2O fully confirm the NR as well as QCM-D observations about the structural stability of DPPC supported bilayers against removal by "Sigma" QBS.

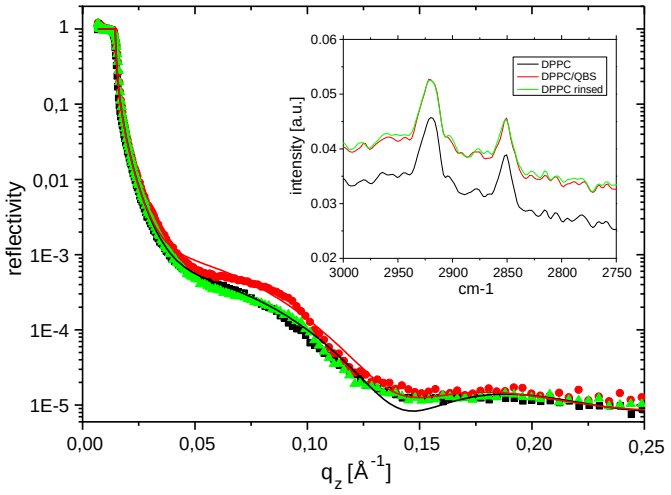

Fig. 9. Neutron reflectivity curves and FTIR ATR spectra (inset) at the Si/water interface (20 °C) of DPPC bilayers in pure D_2O (black squares), DPPC bilayers penetrated with QBS (red circles) and of the same system after exchange of QBS back with D_2O (green triangles). The values of the fit (straight line) are given in the text.

4. Discussion

The distinctly different effects of SDS, CTAB, Triton X-100 and QBS (all above their cmc) on DPPC monolayers compressed to the surface pressure where the molecules in monolayers are believed to exhibit molecular packing similar to that estimated in phospholipid bilayers ($\Pi_0 = 32.5$ mN/m) point to different mechanisms of interaction with DPPC monolayers with these surfactants. Based on the surface pressure relaxation and surface rheological behaviour, they can be classified into three groups:

1) small molecular weight ionic surfactants (CTAB, SDS) capable of quickly incorporating into the monolayer and collapsing it;
2) small molecular weight non-ionic surfactants (Triton X-100) which simply replace the phospholipid on the water surface without any abrupt changes in the surface pressure (without the collapse);
3) higher molecular weight biosurfactants (QBS) capable of incorporating into the monolayer, without disrupting it.

Since the first two groups are well characterised and are beyond the scope of this paper, we focus our attention on QBS. The present observations regarding its interactions with the phospholipid monolayer agree well with the results of Armah et al. for a triterpenoid saponin, avenacin. The latter was found to penetrate the phospholipid monolayers even in the absence of cholesterol, without actually disrupting them [18]. Similar behaviour for silicon-supported DPPC bilayers was reported using neutron reflectivity also for another biosurfactant, surfactin [44],

although only below its cmc. It is worth stressing here that basing solely on the surface pressure relaxation curves, QBS and Triton X-100 would be considered very similar in terms of their interaction with DPPC monolayer (none of them provokes any collapse-related instabilities). Similar conclusions on non-complete replacement of phospholipids by Triton X-100 were reached by several authors [45,46]. Nevertheless, the rheological response of the mixed layer unequivocally proved that contrary to QBS, Triton X-100 almost completely replaced DPPC, eventually resulting in a low surface dilatational visco-elasticity layer. The dilatational properties of this layer are similar to those obtained by collapsing the DPPC monolayer with the ionic synthetic surfactants and are typical for the adsorbed layers composed predominantly of low molecular weight surfactants [47–49].

The penetration of DPPC monolayer by QBS was studied as a function of the initial surface pressure, hence also of the physical state of the monolayer. This effect was quantified using the maximum insertion pressure (MIP) concept [37]. Generally, it is assumed that if MIP lies below the value of the lateral pressure of biological membranes (typically 30–35 mN/m), a given molecule would not be capable of penetrating the real bilayer membrane. For the DPPC/QBS system MIP = 57.3 mN/m was found by extrapolation of the experimental data, suggesting that QBS penetration into DPPC monolayers is very favourable and can proceed even at very high lateral pressures. Despite distinct improvement of the dilatational visco-elasticity of DPPC layers penetrated by QBS, no clear change can be seen in the layer structure, as evidenced by neutron reflectometry (NR, Fig. 7).

NR did not reveal significant alterations in the structure of DPPC bilayers upon exposure to QBS, either. The most important conclusion from the combined NR/IR study of the supported bilayers is that QBS does not remove the phospholipid, even after subsequent rinsing with water. The adsorbed mass analysis using QCM-D proven more quantitative in this respect. The profile of the frequency change in the experiment shown in Fig. 8 suggests that QBS adsorbs readily onto the DPPC bilayer, but can also undergo partial desorption upon washing-off. Since the dissipation parameter increased during QBS incorporation, the visco-elastic modelling was employed for calculating the mass density changes of the adsorbed material during this process. After washing off the excess DPPC material adsorbed onto its bilayer, the mass density of the adsorbed phospholipid (at t = 80 min, Fig. 8) was 439 ng/cm^2. This corresponds well with the mass densities reported typically for SLBs of PC phospholipids (420–440 ng/cm^2) [50,51]. The mass densities of the adsorbed material after incorporation of QBS (t = 130 min) and after the subsequent washing off (t = 160 min) were 652 and 600 ng/cm^2, respectively. Clearly, the mass of the adsorbed material has greatly increased after exposing the DPPC bilayer to the QBS solution. Even though after flushing the cell with pure water some of the material was washed off, the final mass density was still 161 ng/cm^2 higher than that of the pure DPPC bilayer. This corresponds to an irreversible increase of the adsorbed mass by about 1/3 during the contact of DPPC bilayer with QBS. In our previous paper we found that in the absence of DPPC, QBS shows very little affinity to the bare silicon interface, and the maximum mass density achievable for the QBS solution of the same concentration is only 60 ng/cm^2 [41]. Therefore, the increase of the adsorbed mass density observed in the system DPPC/QBS must originate from penetration of QBS into the DPPC bilayer, not its replacement and adsorption of QBS onto Si. In our previous study we also found that the QBS adsorbed layers are highly hydrated, e.g., at the water/air interface the mass ratio of QBS/water was only ½ [41]. Therefore, part of the additional mass density brought with QBS during its penetration into the DPPC bilayers may come from water, hence the weak changes observed in NR.

Chemically, saponins are glycosides composed of the aglycone (triterpenoid or steroid) and the (oligo)sugar (glycone) parts. In this context it is interesting to compare the mode of action of the aglycone and glycone moieties with that of the glycosides. In the case of QBS, the aglycone part is typically a triterpenoid one [52]. The free triterpenic acids were shown to only slightly alter the structural order of model DPPC multilayers, without destabilizing them [53]. Based on an extensive calorimetric, X-ray diffraction, ^{31}P NMR and fluorimetric study, the authors concluded that the free triterpenic acids locate themselves close to the lipid head groups. Similarly, the lupane-type pentacyclic triterpenes were shown to mix well with DPPC monolayers, lowering their periodical order [54]. Sterols (e.g., cholesterol), which also bear some structural similarity to aglycone parts of saponins (especially the steroid ones) are known to condense and increase the order of the phospholipid layers [55,56].

On the other hand, sugars usually have the opposite effect on phospholipid membranes: they expand the monolayers [38,57] by partially replacing water from the hydration shell of the phospholipid head groups [58,59]. The loss of van der Waals attraction between the closely packed acyl chains in the sugar-penetrated phospholipid membranes is compensated by formation of hydrogen bonds between the sugar and the water hydrating phospholipid head groups [60]. Consequently, upon increasing lateral pressure in a sugar-penetrated monolayer, the sugar can be easily expelled from DPPC monolayers into the subphase [38].

The strong effect of “Sigma” QBS on DPPC monolayer surface pressure and surface dilatational visco-elasticity modulus observed in our study might be interpreted as resulting from the insertion of both the aglycone and glycone parts of the saponin molecules into the phospholipid monolayer. The interactions between the two molecules in the monolayer are so strong that QBS never expels DPPC from the surface, even after collapsing the monolayer (Fig. 5e, Π_0 = 51 mN/m). Recently Golemanov et al. interpreted an unusually high surface shear visco-elasticity of different triterpene saponins as resulting from an extensive hydrogen bond network formation involving the sugar parts in the adsorbed layers [61]. As proven by the comparison of the effect of QBS and pure sugars on DPPC monolayers compressed to Π_0 = 32.5 mN/m, the sugar moieties alone do not provide sufficient anchor to the phospholipid layer. Only with help of an additional interaction, provided by the aglycone part, they can effectively incorporate into the phospholipid layer.

5. Conclusions

Using a combination of surface pressure relaxation and dilatational surface rheology we showed that the penetration of the compressed DPPC monolayer by QBS clearly proceeds via different mechanism than for typical synthetic surfactants, both non-ionic (Triton X-100), and ionic: SDS (anionic) and CTAB (cationic). In contrast to the synthetic surfactants, QBS is capable to insert into the monolayer increasing the surface pressure and enhancing its dilatational visco-elastic properties. Even at very high surface pressures the DPPC monolayer is not collapsed by QBS, and the estimated maximum insertion pressure (MIP) exceeds that of the maximum surface pressure achievable in our setup for pure DPPC. The experiments with DPPC bilayers deposited on silicon surface using NR and QCM-D also confirm the strong penetrating ability of QBS. The fact that the QBS-penetrated DPPC layers experience higher surface pressure and display stronger dilatational elastic character, despite the layer thickness not being altered, suggests that QBS is located in the plane of DPPC layers. In other words, in both mono- and bilayers QBS has proven to effectively penetrate the phospholipid layers, strengthening them instead of disrupting, as it is the case for the synthetic low molecular weight surfactants.

Despite several attempts to correlate the hemolytic and cytotoxic activity with structure of both glycone and aglycone parts of saponins [1,62–65], still not much is known about the respective roles of each of the two parts in interaction with biological membranes. Therefore, the penetration observed in this study does not have to be an universal feature of all phospholipid-saponin interactions and require further studies with other saponins and lipids.

Acknowledgements

This work was financially supported by the Polish National Science Centre, grant no. DEC-*2011/03/B/ST4/00780* and COST CM1101 Action. Part of this work is based on experiments performed at the Swiss spallation neutron source SINQ, Paul Scherrer Institute, Villigen, Switzerland. Allocation of neutron beam time at the research reactor BER II at HZB is gratefully acknowledged.

Appendix A. Supplementary data

Supplementary data to this article can be found online at http://dx.doi.org/10.1016/j.bbamem.2014.04.008.

References

[1] Y. Wang, Y. Zhang, Z. Zhu, S. Zhu, Y. Li, M. Li, B. Yu, Bioorg. Med. Chem. 15 (2007) 2528–2532.
[2] S. Guo, K. Lennart, L.N. Lundgren, B. Rönnberg, B.G. Sundquist, Phytochemistry 48 (1998) 175–180.
[3] A. Osbourn, R.J. Goss, R.A. Field, Nat. Prod. Rep. 28 (2011) 1261–1268.
[4] R. San Martín, R. Briones, Econ. Bot. 53 (1999) 302–311.
[5] Ö. Güçlü-Üstündağ, G. Mazza, Crit. Rev. Food Sci. Nutr. 47 (2007) 231.
[6] L.I. Nord, L. Kenne, Carbohydr. Res. 320 (1999) 70–81.
[7] K. Wojciechowski, Colloids Surf. B: Biointerfaces 108 (2013) 95–102.
[8] J.L. Cleland, C.R. Kensil, A. Lim, N.E. Jacobsen, L. Basa, M. Spellman, D.A. Wheeler, J. Wu, M.F. Powell, J. Pharm. Sci. 85 (1996) 22–28.
[9] E. Wina, S. Muetzel, K. Becker, J. Agric. Food Chem. 53 (2005) 8093–8105.
[10] G.S. Sidhu, D.G. Oakenfull, Br. J. Nutr. 55 (1986) 643–649.
[11] A. Weng, C. Bachran, H. Fuchs, M.F. Melzig, Chem. Biol. Interact. 176 (2008) 204–211.
[12] A. Weng, M. Thakur, B. Von Mallinckrodt, F. Beceren-Braun, R. Gilabert-Oriol, B. Wiesner, J. Eichhorst, S. Böttger, M.F. Melzig, H. Fuchs, J. Control. Release 164 (2012) 74–86.
[13] J.M. Gee, J.M. Wal, K. Miller, H. Atkinson, F. Grigoriadou, M.V.W. Wijnands, A.H. Penninks, G. Wortley, I.T. Johnson, Toxicology 117 (1997) 219–228.
[14] F.M. Menger, J.S. Keiper, Angew. Chem. Int. Ed. 37 (1999) 3433–3435.
[15] J.M. Augustin, V. Kuzina, S.B. Andersen, S. Bak, Phytochemistry 72 (2011) 435–457.
[16] E.A.J. Keukens, T. De Vrije, L.A.M. Jansen, H. De Boer, M. Janssen, A.I.P.M. De Kroon, W.M.F. Jongen, B. De Kruijff, Biochim. Biophys. Acta Biomembr. 1279 (1996) 243–250.
[17] E.A.J. Keukens, T. De Vrije, C. Van den Boom, P. De Waard, H.H. Plasman, F. Thiel, V. Chupin, W.M.F. Jongen, B. De Kruijff, Biochim. Biophys. Acta Biomembr. 1240 (1995) 216–228.
[18] C.N. Armah, A.R. Mackie, C. Roy, K. Price, A.E. Osbourn, P. Bowyer, S. Ladha, Biophys. J. 76 (1999) 281–290.
[19] M. Hu, K. Konoki, K. Tachibana, Biochim. Biophys. Acta Lipids Lipid Metab. 1299 (1996) 252–258.
[20] J.H. Schulman, E.K. Rideal, Proc. R. Soc. Lond. Ser. B Biol. Sci. 122 (1937) 29–45, http://dx.doi.org/10.1098/rspb.1937.0008.
[21] J. Goerke, Biochim. Biophys. Acta Mol. Basis Dis. 1408 (1998) 79–89.
[22] S. Engelskirchen, Curr. Opin. Colloid Interface Sci. 12 (2007) 68–74.
[23] E.H. Lucassen-Reynders, Surfactant Sci. Ser. 11 (1981) 173–216.
[24] M. Gupta, T. Gutberlet, J. Stahn, P. Keller, D. Clemens, Pramana -J. Phys. 63 (2004) 57–63.
[25] M. Strobl, R. Steitz, M. Kreuzer, M. Rose, H. Herrlich, F. Mezei, M. Grunze, R. Dahint, Rev. Sci. Instrum. 82 (2011) 055101-1.
[26] A.A. van Well, Phys. B Condens. Matter 180–181 (1992) 959–961.
[27] U. Mennicke, T. Salditt, Langmuir 18 (2002) 8172–8177.
[28] M. Kreuzer, M. Strobl, M. Reinhardt, M.C. Hemmer, T. Hauß, R. Dahint, R. Steitz, Biochim. Biophys. Acta Biomembr. 2012 (1818) 2648–2659.
[29] C. Braun, Experimental report HMI: Berlin, 1999.
[30] L.G. Parratt, Phys. Rev. 95 (1954) 359–369.
[31] R.P. Richter, R. Bérat, A.R. Brisson, Langmuir 22 (2006) 3497–3505.
[32] T.H. Anderson, Y. Min, K.L. Weirich, H. Zeng, D. Fygenson, J.N. Israelachvili, Langmuir 25 (2009) 6997–7005.
[33] O.G. Travkova, G. Brezesinski, Chem. Phys. Lipids 167–168 (2013) 43–50.
[34] D. Marsh, Biochim. Biophys. Acta Rev. Biomembr. 1286 (1996) 183–223.
[35] F. Miano, C.P. Winlove, D. Lambusta, G. Marletta, J. Colloid Interface Sci. 296 (2006) 269–275.
[36] A.L. Caro, M.R.R. Niño, J.M.R. Patino, Colloids Surf. A Physicochem. Eng. Asp. 332 (2009) 180–191.
[37] P. Calvez, S. Bussières, Éric Demers, C. Salesse, Biochimie 91 (2009) 718–733.
[38] N. Krasteva, D. Vollhardt, G. Brezesinski, H. Möhwald, Langmuir 17 (2001) 1209–1214.
[39] K. Wojciechowski, M. Piotrowski, W. Popielarz, T.R. Sosnowski, Food Hydrocoll. 25 (2011) 687–693.
[40] F. Miano, X. Zhao, J.R. Lu, J. Penfold, Biophys. J. 92 (2007) 1254–1262.
[41] K. Wojciechowski, M. Orczyk, K. Marcinkowski, T. Kobiela, M. Trapp, T. Gutberlet, T. Geue, Colloids Surf. B 117 (2014) 60–67.
[42] R. Richter, A. Mukhopadhyay, A. Brisson, Biophys. J. 85 (2003) 3035–3047.
[43] B. Scantier, C. Breffa, O. Félix, G. Decher, J. Phys. Chem. B 109 (2005) 21755–21765.
[44] H. Shen, R.K. Thomas, J. Penfold, G. Fragneto, Langmuir 26 (2010) 7334–7342.
[45] B. Hu, L. Mi, S. Sui, Thin Solid Films 327–329 (1998) 69–73.
[46] P. Fontaine, M.C. Fauré, F. Muller, M. Poujade, J. Micha, F. Rieutord, M. Goldmann, Langmuir 23 (2007) 12959–12965.
[47] L. Liggieri, M. Ferrari, D. Mondelli, F. Ravera, Faraday Discuss. 129 (2005) 125–140.
[48] R. Miller, V.B. Fainerman, J. Kragel, L. Guiseppe, Curr. Opin. Colloid Interface Sci. 2 (1997) 578–583.
[49] R. Miller, M.E. Leser, M. Michel, V.B. Fainerman, J. Phys. Chem. B 109 (2005) 13327–13331.
[50] S. Boudard, B. Seantier, C. Breffa, G. Decher, O. Félix, Thin Solid Films 495 (2006) 246–251.
[51] K. Morigaki, S. Kimura, K. Okada, T. Kawasaki, K. Kawasaki, Langmuir 28 (2012) 9649–9655.
[52] J. Vincken, L. Heng, A. de Groot, H. Gruppen, Phytochemistry 68 (2007) 275–297.
[53] J. Prades, O. Vögler, R. Alemany, M. Gomez-Florit, S.S. Funari, V. Ruiz-Gutiérrez, F. Barceló, Biochim. Biophys. Acta Biomembr. 2011 (1808) 752–760.
[54] M. Broniatowski, M. Flasinski, P. Wydro, J. Colloid Interface Sci. 381 (2012) 116–124.
[55] T. Róg, M. Pasenkiewicz-Gierula, I. Vattulainen, M. Karttunen, Biochim. Biophys. Acta Biomembr. 1788 (2009) 97–121.
[56] H.P. Vacklin, F. Tiberg, G. Fragneto, R.K. Thomas, Langmuir 21 (2005) 2827–2837.
[57] S. Nakata, T. Shiota, N. Kumazawa, M. Denda, Colloids Surf. A Physicochem. Eng. Asp. 405 (2012) 14–18.
[58] C.S. Pereira, P.H. Hünenberger, J. Phys. Chem. B 110 (2006) 15572–15581.
[59] S. Leekumjorn, A.K. Sum, J. Phys. Chem. B 112 (2008) 10732–10740.
[60] J.H. Crowe, L.M. Crowe, D. Chapman, Science 223 (1984) 701–703.
[61] K. Golemanov, S. Tcholakova, N. Denkov, E. Pelan, S.D. Stoyanov, Soft Matter 9 (2013) 5738–5752.
[62] D.J. Pillion, J.A. Amsden, C.R. Kensil, J. Recchia, J. Pharm. Sci. 85 (1996) 518–524.
[63] M. Chwalek, N. Lalun, H. Bobichon, K. Plé, L. Voutquenne-Nazabadioko, Biochim. Biophys. Acta Gen. Subj. 1760 (2006) 1418–1427.
[64] C. Gauthier, J. Legault, K. Girard-Lalancette, V. Mshvildadze, A. Pichette, Bioorg. Med. Chem. 17 (2009) 2002–2008.
[65] S. Böttger, K. Hofmann, M.F. Melzig, Bioorg. Med. Chem. 20 (2012) 2822–2828